Faraday rotation of spontaneous magnetization in a laserproduced plasma from solid target

Manoranjan Khan, Susmita Sarkar, B. Bhattacharyya, B. Chakraborty, T. Desai, and H. C. Pant

Citation: Journal of Applied Physics **72**, 2144 (1992); doi: 10.1063/1.351602
View online: http://dx.doi.org/10.1063/1.351602
View Table of Contents: http://scitation.aip.org/content/aip/journal/jap/72/6?ver=pdfcov
Published by the AIP Publishing

Faraday rotation of spontaneous magnetization in a laser-produced plasma from solid target

Manoranjan Khan, Susmita Sarkar, B. Bhattacharyya, and B. Chakraborty
Plasma Physics Group, Department of Mathematics, Jadavpur University, Calcutta-700032, India

T. Desai[a] and H. C. Pant
Laser and Plasma Technology Division, Bhabha Atomic Research Centre, Bombay-400085, India

(Received 27 September 1991; accepted for publication 11 May 1992)

Interaction of elliptically polarized laser radiation with plasma produced from a solid target generates magnetic fields simultaneously along axial and transverse directions. The axial magnetic field induces the plane of polarization of the incident laser beam to rotate due to the Faraday effect. Numerically the Faraday rotation has been calculated for interaction of Nd glass laser ($\lambda=1.06$ μm) in the subdense plasma in which the plasma density, temperature, and self-generated magnetic field vary in the axial direction.

I. INTRODUCTION

In schemes of fusion reaction by inertial confinement, a self-generated magnetic field is found to influence the energy transport, and hence the pellet design; thus, this magnetic-field generation becomes the motivation for many expeirmental and theoretical studies.

Several independent mechanisms are known[1-9] to be responsible for the generation of laser-induced toroidal magnetic fields. These fields are either of a large scale or of a small scale. Known sources of laser-induced large-scale magnetic fields are (i) the $\nabla n\times\nabla T$ mechanism,[1,2,5] (ii) anisotropy of electron plasma,[3] and (iii) hot-electron ejection from the focal spot.[4] These large-scale torodial fields are ordered fields. There have been quite a few proposals of mechanism for the B field with small spatial scales, ranging from a few vacuum laser wave lengths to an electron mean free path. Since these fields lack large-scale coherence, these small-scale toroidal magnetic fluctuations may have a significant effect on the electron transport coefficients. Sources of small-scale magnetic field are (i) filamentation,[5] (ii) resonance absorption,[6] (iii) thermal instabilities,[7] and (iv) Weibel instabilities.[8] However, the self-generated axial magnetic field was not reported till Briand *et al.*[10] proposed that an axial magnetic field can grow up from these small-scale magnetic fields through the dynamo effect. Furthermore, they presented an experiment which showed than an axial magnetic field of 0.6 MG exists in a plasma produced by the interaction of an intense 0.53 μm laser beam with a plane target. However, the demonstration given by Briand *et al.* was shown to be unacceptable by Dragila[11] who suggested that in underdense plasmas a turbulent dynamo effect is possibly responsible for the generation of axial magnetic fields observed in laser-produced plasma in the presence of ion-acoustic turbulence. Moreover, it leads to enhancement of the original toroidal magnetic field generated by the $\nabla n\times\nabla T$ mechanism. Chakraborty, Khan and Bhattacharyya[12] have suggested yet another mechanism for the generation of an axial magnetic field of appreciable magnitude. This type of field is investigated in the interaction of standing waves in a laser-produced plasma neglecting the plasma temperature. A knowledge of the scaling laws with induced magnetization for different laser powers and wave lengths and with different plasma densities has also been reported subsequently by Chakraborty *et al.*[13]

In this paper we present a theory for the simultaneous generation of both axial and lateral magnetic fields in a highly collisional, hot, homogeneous plasma, produced by interaction of an intense laser beam with a solid target. This induced magnetization is a modified inverse Faraday effect of interaction of dispersive transverse and longitudinal waves of the same frequency in a plasma. As in the usual inverse Faraday effect, here also the kinetic energy of ordered motion of charges in the presence of waves is transformed into the energy of the induced magnetic field. The ordered motion of the charged particles, due to this wave, gives rise to a static magnetic moment along the axial and lateral directions, which obtains from averaging that expression over the wave time periods.

II. FORMULATION OF THE PROBLEM

The plasma is assumed to be a hot, adiabatic, and homogeneous fluid, and is highly collisional. The high collisionality gives rise to only randomization of energy which leads to equalization of electron and ion temperatures (i.e., $T_e\approx T_i$), but does not lead to any appreciable dissipation of energy.

The following set of equations is assumed to describe the interaction of the laser beam with the plasma:

$$\dot{N}+\nabla\cdot(N\dot{\mathbf{r}})=0, \tag{1}$$

$$\ddot{\mathbf{r}}+(\dot{\mathbf{r}}\cdot\nabla)\dot{\mathbf{r}}+\frac{e}{m}\mathbf{E}+\frac{e}{mc}(\dot{\mathbf{r}}\times\mathbf{H})+\frac{\nabla p}{mN}=0, \tag{2}$$

$$\nabla\times\mathbf{E}=-\frac{1}{c}\dot{\mathbf{H}}, \tag{3}$$

$$\nabla\times\mathbf{H}=\frac{1}{c}\dot{\mathbf{E}}-\frac{4\pi e}{c}N\dot{\mathbf{r}}, \tag{4}$$

[a]Present address: Laser Fusion Programme, Centre of Advanced Technology, Indore, India.

 0021-8979/92/182144-05$04.00

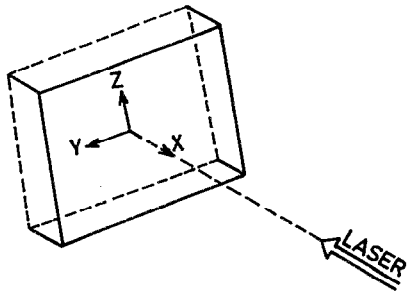

FIG. 1. The target coordinate axes impinging the laser beam.

$$\nabla\cdot\mathbf{E}=-4\pi e(N-N_0), \tag{5}$$

$$\nabla\cdot\mathbf{H}=0. \tag{6}$$

The notations have their usual meanings for motion of electrons of charge $-e$ and mass m. The elliptically polarized electric field is of the form

$$\mathbf{E}_1=\frac{mc\omega}{e}(\alpha_\parallel\cos\theta_\parallel,\alpha_\perp\cos\theta_\perp,\beta_\perp\sin\theta_\perp), \tag{7}$$

where $\theta_\parallel=k_\parallel x-\omega t$, $\theta_\perp=k_\perp x-\omega t$. At $x=0$, the transverse oscillation in the X-Y plane is assumed to be in phase with the longitudinal oscillation and the transverse oscillation in the X-Z plane is out of phase with the longitudinal oscillation by $\pi/2$ (Fig. 1).

The excited fields, evaluated from the linearized approximation of the field equations, are

$$\mathbf{H}_1=\frac{mc\omega}{e}n_\perp(0,-\beta_\perp\sin\theta_\perp,\alpha_\perp\cos\theta_\perp), \tag{8}$$

$$\dot{\mathbf{r}}_1=\frac{c}{X}(\alpha_\parallel\sin\theta_\parallel,X\alpha_\perp\sin\theta_\perp,-X\beta_\perp\cos\theta_\perp), \tag{9}$$

$$N_1=\frac{N_0}{X}\alpha_\parallel n_\parallel\sin\theta_\parallel. \tag{10}$$

The linearized dispersion relations for the transverse wave and longitudinal wave, respectively, are

$$n_\perp^2-1+X=0,\quad n_\parallel^2\frac{\gamma v_{\rm th}^2}{c^2}=1-X, \tag{11}$$

where

$$n_\parallel=\frac{k_\parallel c}{\omega},\quad n_\perp=\frac{k_\perp c}{\omega},\quad \alpha_\parallel=\frac{ea_\parallel}{mc\omega},$$

$$(\alpha_\perp,\beta_\perp)=\frac{e(a_\perp,b_\perp)}{mc\omega},\quad X=\frac{\omega_p^2}{\omega^2},$$

and γ is the ratio of two specific heats. Similarly, the second-order fields have also been obtained from the same set of equations.

Using these field variables we obtain the following inhomogeneous, nonlinear, third-order wave equation:

$$c^2\,\text{grad div}\,\mathbf{E}_3-c^2\nabla^2\mathbf{E}_3+\ddot{\mathbf{E}}_3+\omega_p^2\mathbf{E}_3-\frac{\gamma v_{\rm th}^2}{2}\,\text{grad div}\,\mathbf{E}_3$$

$$=4\pi eN_0\Big[-(\dot{\gamma}_2\cdot\nabla)\dot{\mathbf{r}}_1-(\dot{\gamma}_1\cdot\nabla)\dot{\gamma}_2-\frac{e}{mc}(\dot{\gamma}_1\times\mathbf{H}_2)$$

$$-\frac{e}{mc}(\dot{\gamma}_2\times\mathbf{H}_1)-\frac{\gamma v_{\rm th}^2}{2N_0^3}N_1^2\nabla N_1+\frac{\gamma v_{\rm th}^2}{2N_0^2}N_1\nabla N_2$$

$$+\frac{\gamma v_{\rm th}^2}{2N_0^2}N_2\nabla N_1+\frac{1}{N_0}D(N_2\dot{\gamma}_1+N_1\dot{\gamma}_2)\Big], \tag{12}$$

where the inhomogeneity, collected in the right-hand side, is exclusively due to nonlinearity.

Solving the nonlinear equation (12) for secular-free solution and retaining only the first harmonic terms, correct up to the third order, we obtain the following expressions for the nonlinear increments of the electron velocity and the corresponding displacements:

$$\dot{\gamma}_3=2c\{\hat{x}[-\kappa_1\alpha_\parallel^2\sin\theta_\parallel-\kappa_2(\alpha_\perp^2-\beta_\perp^2)\sin\theta_{\perp,\parallel}-\kappa_3(\alpha_\perp^2+\beta_\perp^2)\sin\theta_\parallel]\alpha_\parallel+\hat{y}[-\Sigma_1\alpha_\parallel^2\sin\theta_{\parallel,\perp}-\Sigma_2(\alpha_\perp^2-\beta_\perp^2)\sin\theta_\perp$$
$$-\Sigma_3\alpha_\parallel^2\sin\theta_\perp]\alpha_\perp+\hat{z}[-\Sigma_1\alpha_\parallel^2\cos\theta_{\parallel,\perp}-\Sigma_2(\alpha_\perp^2-\beta_\perp^2)\cos\theta_\perp+\Sigma_3\alpha_\parallel^2\cos\theta_\perp]\beta_\perp\}, \tag{13}$$

$$\gamma_3=-\frac{2c}{\omega}\{\hat{x}[\kappa_1\alpha_\parallel^2\cos\theta_\parallel+\kappa_2(\alpha_\perp^2-\beta_\perp^2)\cos\theta_{\perp,\parallel}+\kappa_3(\alpha_\perp^2+\beta_\perp^2)\cos\theta_\parallel]\alpha_\parallel+\hat{y}[\Sigma_1\alpha_\parallel^2\cos\theta_{\parallel,\perp}+\Sigma_2(\alpha_\perp^2-\beta_\perp^2)\cos\theta_\perp$$
$$+\Sigma_3\alpha_\parallel^2\cos\theta_\perp]\alpha_\perp+\hat{z}[-\Sigma_1\alpha_\parallel^2\sin\theta_{\parallel,\perp}-\Sigma_2(\alpha_\perp^2-\beta_\perp^2)\sin\theta_\perp-\Sigma_3\alpha_\parallel^2\sin\theta_\perp]\beta_\perp\}, \tag{14}$$

where

$$\theta_{\parallel,\perp}=(2k_\parallel-k_\perp)x-\omega t,\quad \theta_{\perp,\parallel}=(2k_\perp-k_\parallel)x-\omega t,$$

$$\kappa_1=-\left(\tau_\parallel+\frac{2\delta n_\parallel}{X}+-\frac{n_\parallel^2}{8X^3}\right),$$

$$\kappa_2=-\left(\tau_{22}-\frac{Q}{X}(n_\parallel+n_\perp)\right),$$

$$\kappa_3=-n_\parallel[-X(n_\parallel+n_\perp)+2n_\perp]\Big/$$

$$8X\left\{\frac{\gamma v_{\rm th}^2}{2c^2}(n_\parallel+n_\perp)^2-4+X\right\}\left\{X-1+\frac{\gamma v_{\rm th}^2}{2c^2}n_\parallel^2\right\},$$

$$\Sigma_1=\delta n_\parallel\left[\frac{(2n_\parallel-n_\perp)^2-1}{X-1+\gamma v_{\rm th}^2/(2c^2 2n_\parallel-n_\perp)^2}-1\right],$$

$$\Sigma_2=Qn_\perp\left[\frac{X}{X-1+\gamma v_{\rm th}^2/2c^2 n_\perp^2}+1\right],$$

$$\Sigma_3=n_\parallel(n_\parallel+n_\perp)\Big/8\left\{X-1+\frac{\gamma v_{\rm th}^2}{2c^2}n_\perp^2\right\}$$
$$\times\left\{\frac{\gamma v_{\rm th}^2}{2c^2}(n_\parallel+n_\perp)^2-4+X\right\}$$
$$-\frac{n_\parallel}{8X^2}\left[\frac{2\{1-\frac{1}{2}(n_\parallel+n_\perp)^2\}}{\gamma v_{\rm th}^2/2c^2(n_\parallel+n_\perp)^2-4+X}+1\right]$$
$$\times\left[n_\parallel+\frac{X(2n_\parallel+n_\perp)}{X-1+\frac{\gamma v_{\rm th}^2}{2c^2}n_\perp^2}\right],$$

$$\tau_\parallel=\left[\frac{4n_\parallel\delta}{X}+\frac{n_\parallel^2}{2X^3}-\frac{\gamma v_{\rm th}^2}{2c^2X}n_\parallel^3\left(\delta+\frac{n_\parallel}{8X^2}\right)\right]\Big/$$
$$\left[X-1+\frac{\gamma v_{\rm th}^2}{2c^2}n_\parallel^2\right],$$

$$\tau_{22}=\left[-\frac{2Qn_\perp^2}{X}+\frac{\gamma v_{\rm th}^2}{2Xc^2}Qn_\parallel n_\perp(2n_\perp-n_\parallel)\right]\Big/$$
$$\left[X-1+\frac{\gamma v_{\rm th}^2}{2c^2}(2n_\perp-n_\parallel)^2\right], \qquad (15)$$

$$\delta=\frac{n_\parallel}{4X^2}\left(3-\frac{\gamma v_{\rm th}^2}{2c^2}n_\parallel^2\right)\Big/\left(\frac{2\gamma v_{\rm th}^2}{c^2}n_\parallel^2-4+X\right),$$

$$Q=-n_\perp\Big/4\left\{\frac{2\gamma v_{\rm th}^2}{c^2}n_\perp^2-4+X\right\}.$$

The nonlinear magnetization, induced in the laser-produced plasma, averaged over the wave time period, is

$$\langle M\rangle=(4\pi Ne/c)\langle L\rangle, \qquad (16)$$

where $\langle L\rangle$ is the time-averaged angular momentum gained. The components of the nonlinear angular momentum are

$$L_x=\frac{4c^2}{\omega}\{[\Sigma_1\alpha_\parallel^2+\Sigma_2(\alpha_\perp^2-\beta_\perp^2)]^2-\Sigma_3^2\alpha_\parallel^4\}\alpha_\perp\beta_\perp,$$

$$L_y=-\frac{4c^2}{\omega}[\Sigma_1\alpha_\parallel^2+\Sigma_2(\alpha_\perp^2-\beta_\perp^2)-\Sigma_3\alpha_\parallel^2]$$
$$\times[\kappa_1\alpha_\parallel^2+\kappa_2(\alpha_\perp^2-\beta_\perp^2)+\kappa_3(\alpha_\perp^2+\beta_\perp^2)]\alpha_\parallel\beta_\perp, \qquad (17)$$

$$L_z=0.$$

Hence, the magnetization is nonzero along X and Y directions, which are, respectively, the axial direction and a laterial direction, but along the Z axis it is zero. The magnitude and direction of this induced magnetization depends on the phase relation between the longitudinal wave and transverse oscillations along the two principal directions of the polarization ellipse of the electromagnetic wave. For instance, in the spatial evolution problems, the induced magnetization vanishes along the direction of transverse oscillation, the phase of which oscillation at the boundary $x=0$ differs perfectly by the angle $\pi/2$ with the phase of the longitudinal wave there. Thus, the resultant magnetic field lies in the X-Y plane.

This axial magnetic field induces the plane of polarization of the incident laser beam to rotate due to the Faraday effect. This rotation occurs in the subdense plasma in which the plasma density, temperature, and self-generated magnetic field vary in the axial direction. For convenience, the space has been divided into a finite number of slabs along the axial direction. In each slab the density and hence the magnetic field are assumed to be fairly constant in space. The total Faraday rotation in the whole space is taken as the sum total of the Faraday rotation caused by each slab. The net rotation is then taken as $\alpha=\Sigma_{l=1}^{q}\Delta\alpha_l$, where $\Delta\alpha_l(=B_l\Delta R_l)$ is the rotation due to the lth slab, B_l being the corresponding axial magnetic field in the mega-Gauss units, ΔR_l is the slab thickness in micrometers, and q is a finite number.

III. RESULTS AND DISCUSSIONS

For estimating the self-generated axial magnetic field, steady-state profiles of the plasma corona were estimated using the usual density profile and temperature profile shown in Figs. 2 and 3. Laser absorption in various space regimes of the plasma corona was also estimated from Table I.

A numerical estimation of the magnetic field was made at an absorbed laser intensity of 5×10^{12} W/cm^2. Thermal energy was obtained from the expression $5(2+1/Z)NKT(\Delta R/2\tau)$, where Z, KT, τ, N, and ΔR are the effective ion charge, electron temperature, laser pulse duration, electron density, and length of the plasma slab in the corona, respectively. The calculated axial magnetic field in various slabs along the corona is given in Table I. The axial magnetic field has been observed to be very small

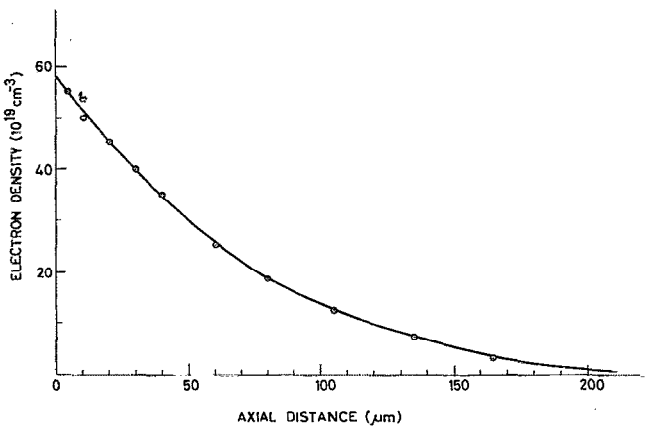

FIG. 2. Variation of electron density with axial distance from the critical density surface.

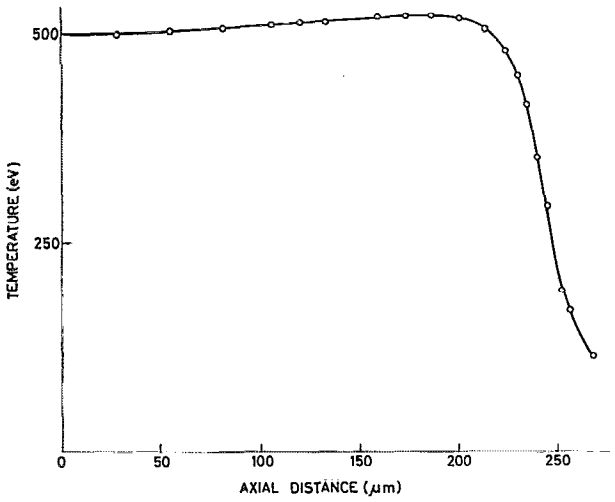

FIG. 3. Variation of temperature (in eV) with axial distance from the critical density surface.

near the critical density layer but is found to have a maximum value of 7464 G at a density of 10^{19} electrons cm^{-3} at a distance of 210 μm from the critical density surface.

Table I shows that the effective value of the axial magnetic field increases from 0.031 G to 7.464 kG when the laser absorption decreases from 75% to 4%. Table I also shows the axial and transverse magnetization in each plasma slab in the plasma corona. Net Faraday rotation is thus calculated by summing up the rotation produced by each slab. The total length of the corona considered for the calculation is 210 μm. Net rotation thus comes to be 5.4° for a single pass of the laser. For the double pass (back reflection) the rotation would thus be 10.8°. In the computed Faraday rotation angle ($=\Sigma_{l=1}^{q} B_l \Delta R_l$), we have restricted our calculation up to a distance of 210 μm from the critical density surface due to the following reasons. The entire region under consideration is divided into some slabs; the length ΔR of each slab is so chosen, that the temperature is seen to be fairly constant in each slab, and the mean value of density is taken. The induced magnetic field is calculated on the basis of these values of temperature and density; consequently, the product $B_l \Delta R_l$ is calculated over each slab, B_l is seen to be fairly constant over the slab length.

As we have already mentioned, beyond 210 μm, it is observed from Figs. 1 and 2 that the temperature is rapidly decaying over the region whereas the density is decaying rather slowly. Thus, it is difficult to choose a slab length, even in the order of 5 μm, over which the mean value of temperature and density may be reasonably chosen. Moreover, the percentage of absorbed laser intensity becomes very small (1%–2%) below the density $10^{19}/cm^3$. Therefore, not only should the calculated axial B_l field over a narrow slab length ΔR_l be small, the product $B_l \Delta R_l$ should be also very small and the finite sum $\Sigma_{l=1}^{q} B_l \Delta R_l$ in this region can be neglected.

A typical calculation has been done for B_l over a slab length $\Delta R_l \sim 5$ μm, $T_e \sim 340$ eV; the percentage of absorbed laser intensity is 1.5, density $0.4 \times 10^{19}/cm^3$. The calculated B_l is of the order of 200 G and $B_l \Delta R_l$ becomes negligible. Hence the contribution of the finite sum $\Sigma B_l \Delta R_l$ to the total Faraday rotation angle over the region is not appreciable. However, where temperature and density gradients are high a toroidal magnetic field (arising from $\nabla n \times \nabla T$) may be generated. But, the Faraday rotation angle of the back-reflected beam is only due to the axial field and thus cannot be affected by the toroidal field.[14]

The self-generated axial magnetic field and the consequent Faraday rotation angle $\Sigma_{l=1}^{q} B_l \Delta R_l$ have been computed here considering the motion of electron to be dominant in laser-produced plasmas.

IV. CONCLUSION

We have shown that the axial and transverse magnetic fields are generated in laser plasma interactions. The transverse field in our problem is exclusively due to the pressure effect in plasma. In a cold plasma, interaction of an electromagnetic wave with the charged particles, rotates the charges in circular orbits and the IFE magnetization obtained is axial and along the line of centers of the circular motion of charges. On the other hand, thermal motion in plasma generates pressure waves which, along with the

TABLE I. Effective values of axial and transverse magnetic field.

Number density ($\times 10^{19}$) (cm^{-3})	Slab length R (μm)	Range (μm)	Intensity ($\times 10^{12}$) (W/cm^2)	% of absorbed intensity	Effective intensity ($\times 10^{12}$) (W/cm^2)	Effective magnetic field along X axis (G)	Magnetic field along Y axis (G)
1	30	180–210	5	4	0.2	7464	-0.9871×10^{3}
3	30	150–180	5	5	0.25	350	-0.2033×10^{2}
7	30	120–150	5	6	0.30	30	-0.9430×10^{0}
12.5	30	90–120	5	9.5	0.475	7.6	-0.1181×10^{0}
18.5	20	70–90	5	15	0.75	1.5	-0.9302×10^{-2}
25	20	50–70	5	21	1.05	0.84	-0.309×10^{-2}
35	20	30–50	5	31	1.55	0.31	-0.7694×10^{-3}
45	20	10–30	5	48	2.40	0.192	-0.3497×10^{-3}
54.5	10	0–10	5	75	3.85	0.031	-0.1484×10^{-4}

pump electromagnetic wave, accelerate the electrons to move in complicated three-dimensional tortuous orbits. Each of these orbits may be considered as a sum of a number of small circles whose line of centers does not lie in the same plane and the generated magnetization will be the cumulative sum of the magnetization due to each of these circular motions of charge. The axial part of the field causes Faraday rotation of the back-reflected laser radiation.

ACKNOWLEDGMENTS

The authors are thankful to Dr. S. V. Lawande of Theoretical Physics Division, BARC, Bombay for some useful suggestions and stimulating discussion. The work has been supported by BRNS, Government of India, under Contract No. 25/2/88-G.

[1] J. A. Stamper, K. Papadopoulos, R. N. Sudan, S. O. Lean, E. A. McLean, and J. M. Dawson, Phys. Rev. Lett. **26**, 1012 (1971).
[2] C. E. Max, W. M. Manheimer, and J. J. Thompson, Phys. Fluids **21**, 128 (1978).
[3] J. A. Stamper and B. H. Ripin, Phys. Rev. Lett. **34**, 138 (1975); P. Mora and R. Pellet, Phys. Fluids **24**, 2219 (1981).
[4] R. Kolodner and E. Yablonovitch, Phys. Rev. Lett. **43**, 1420 (1979); A. Raven, P. T. Rumsby, J. A. Stamper, O. Willi, R. Illingworth, and R. Tharaja, Appl. Phys. Lett. **35**, 526 (1979).
[5] B. Grek, P. Martin, T. W. Johnston, H. Pepin, G. Mitohel, and F. Rheault, Phys. Rev. Lett. **41**, 1811 (1978).
[6] J. A. Stamper and D. A. Tidman, Phys. Fluids **16**, 2004 (1973); I. Bernstein, C. E. Max, and J. J. Thompson, Phys. Fluids **21**, 905 (1978).
[7] D. A. Tidman and R. A. Shanny, Phys. Fluids **17**, 1207 (1974).
[8] T. Okada, T. Yabe, and K. Niu, J. Phys. Soc. Jpn. **43**, 1402 (1977); J. P. Matte, A. Bendib, and J. F. Luclani, Phys. Rev. Lett. **58**, 2067 (1987).
[9] C. E. Max, in *Les. Houches, Session XXXIV, 1980—Interaction Laser Plasma*, edited by R. Balian and J. C. Adams (North-Holland, Amsterdam, 1982), pp. 304–410.
[10] J. Briand, V. Adrian, M. El. Tamer, A. Gomes, Y. Quemendr, J. P. Dinquirard, and J. C. Kieffer, Phys. Rev. Lett. **54**, 38 (1985).
[11] R. Dragila, Phys. Fluids **30**, 925 (1987).
[12] B. Chakraborty, M. Khan, and B. Bhattacharyya, J. Appl. Phys. **59**, 1473 (1986).
[13] B. Chakraborty, M. Khan, B. Bhattacharyya, S. Deb, and H. C. Pant, Phys. Fluids **31**, 1303 (1988).
[14] R. H. Lehmberg and J. A. Stamper, Phys. Fluids **21**, 814 (1978).